A Videogrammetric Technique for Measuring the Vibration Displacement of Stay Cables

ZHOU Xiao-qing [1], WEI Ze-long [2], XIA Yong [2], WU Qing-xiong [2, 3]

1. College of Civil Engineering, Shenzhen University, Shenzhen, China.
2. Department of Civil and Structural Engineering, The Hong Kong Polytechnic University, Hong Kong, China
3. College of Civil Engineering, Fuzhou University, China

E-mail: xqzhou@szu.edu.cn

ABSTRACT

Stay cables in cable-stayed bridges are prone to large amplitude oscillations under external excitations. The vibration of the cables is predominantly measured by using accelerometers to measure the acceleration. The dynamic displacement is then usually obtained indirectly from the double integration of the acceleration data. This paper reports an experimental method of measuring the displacement of stayed cables using a digital video camera. With the newly developed videogrammetric technique, the video clips are transferred into image frames, from which the shape and location of the target are identified. The displacement time history is then captured. The technique is applied to a cable-stayed bridge to measure the dynamic displacement of stay cables. The displacement is compared with the acceleration data in the frequency and time domains. The results show that the displacement measured by the digital video camera is comparable to the counterparts integrated from the acceleration data. The vibration frequencies identified from the acceleration are finally used to estimate the tension forces of the cables. The results show that the tension forces have insignificant changes after one year's operation.

KEYWORDS

Stay cable, vibration, displacement measurement, videogrammetric technique, tension force.

INTRODUCTION

Dynamic testing techniques, which use accelerometers to measure acceleration, have been widely developed and dominate vibration measurement. With these techniques, the dynamic velocity and displacement are usually obtained indirectly from the integration of the acceleration data, which introduces numerical problems such as baseline correction. Instruments that directly measure dynamic displacement include the laser Doppler vibrometer and global positioning systems.

The laser Doppler vibrometer (LDV) is used to make non-contact measurements of the velocity of a surface. The LDV uses the Doppler principle to measure the velocity at the point where the laser beam is directed. The reflected laser light is compared with the incident light in an interferometer to give the Doppler-shifted wavelength. This shifted wavelength provides information on surface velocity in the direction of the incident laser beam. Some of the advantages of the LDV over the accelerometer are that the LDV can be directed at targets that are difficult to access or may be too small or too hot to attach a physical transducer. Abe *et al*.[1] and Kaito *et al*.[2] have applied LDVs to measure the vibration of bridge decks and stay cables.

Recently, the global positioning system (GPS) has been utilised to measure displacement. However, its dynamic accuracy is not high enough in many applications. In addition, the GPS equipment needs to be installed on the object of interest, which is difficult for some objects, such as cables. Recently, non-contact measurement techniques such as the photogrammetry and videogrammetry techniques have been developed with the advance of inexpensive and high-performance charge-coupled-device cameras and associated imaging technologies. Bales[3] applied a close-range photogrammetric technique to several bridges to estimate crack sizes and measure deflection. Li and Yuan[4] developed a 3D photogrammetric vision system consisting of TV cameras and 3D control points for measuring bridge deformation. Olaszek[5] incorporated the photogrammetric principle with the computer vision technique to investigate the dynamic characteristics of bridges. Others applications include References [6 ~ 10].

This study aims to develop a videogrammetric technique to measure the dynamic displacement of stay cables in cable-stayed bridges. With this new approach, a digital video camera alone is used to capture the vibration of the stay cables and no equipment needs to be installed on the cables. The video clips are first transferred into image frames and the shape of the target is then recognized using image analysis. From the continuous image frames, the position and, thus, displacement time history of the cables can be identified. The technique is employed to measure the dynamic displacement of stay cables in a cable-stayed bridge. The results are compared with those using accelerometers.

FIELD MEASUREMENT

The Jing Jiang Bridge

The Jing Jiang bridge measured in this study is a cable-stayed type, located between Jing Jiang City and Quan Zhou City, Fujian Province, China. The bridge has two spans, a 200 m main span and a 165 m side span, as shown in Figs. 1 and 2. The tower is 132 m tall and 107.4 m above the deck level. There are 52 pairs of cables in total, 26 for each plane. The distance between the adjacent cables is seven meters, and the layout of the cables (M1~M26 and S1~S26) is illustrated in Fig. 1.

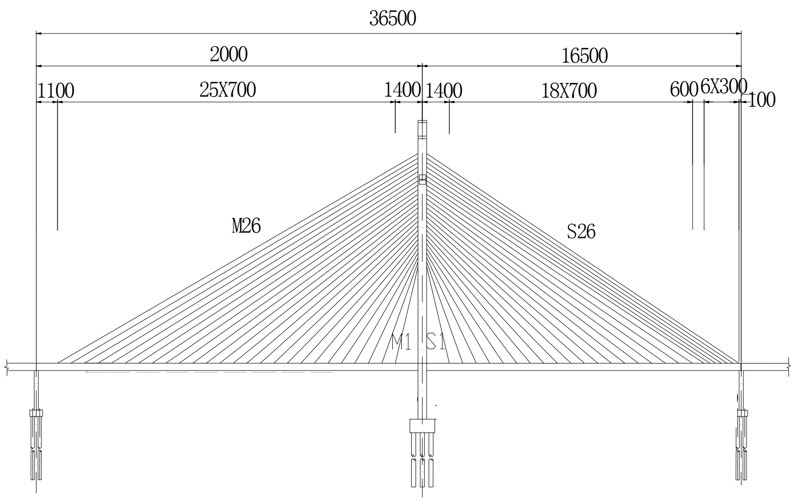

Fig. 1 Configuration of the Jing Jiang Bridge

Fig. 2 View of the Jing Jiang Bridge

Field testing

Large vibration of some of the bridge cables has been observed. This test aims to measure the vibration of the cables using the proposed digital video camera technique in the frequency and time domains and to compare the results with those using conventional accelerometers. The frequency domain data will be used to calculate the tension force of the cables, which will be compared with those measured before the bridge was opened to the public in 2008 [11].

In the experiment in 2009, cable nos. M26 and S25 were measured. Two single-axis accelerometers (type INV9818) were mounted on the cables to measure the acceleration of the cables in the horizontal and transverse directions perpendicular to the longitudinal axis. A digital video camera was used to capture video clips of the target points, which were mounted on the cables a few meters away from the camera. Fig. 3 shows the set-up of the measurement equipment.

Fig. 3 Measurement equipment

Video processing

A video clip is taken of a black solid circle attached to the cable of interest. The motion tracking with the videogrammetric technique includes the following steps.

1. Uncompress the video clip into an uncompressed format, as most video clips are recorded in a compressed format.
2. Transfer the video clip into a series of still images (photos).
3. Identify the shape (circle) in each image.
4. Locate the centroid of the circle.
5. Transfer the motion of the circle in pixel form into that in physical units (meters or mm).

Step 3 above is the key step for obtaining accurate results. A few countermeasures are employed to improve the precision and efficiency of this step:

- The range of the circle is determined beforehand and the later image processing is limited to this area.
- Convert the greyscale image to a binary image, based on the threshold.
- Remove the small objects in the binary image, such that only the target remains.
- Morphologically close the image and smooth the boundary.
- Trace the boundary of the circle.

Fig. 4 illustrates the procedures for processing the still images.

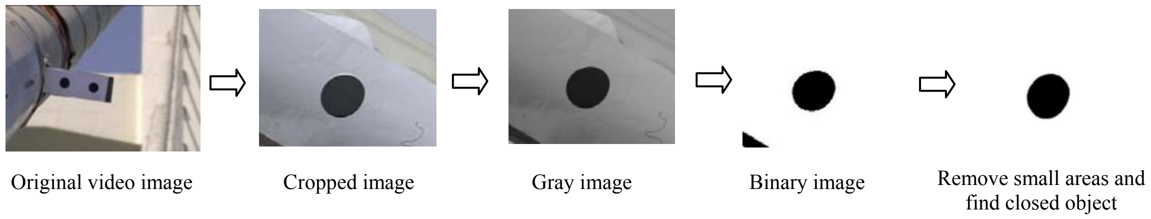

Fig. 4 The image processing procedures

Experimental results

Fig. 4 shows the measured acceleration and power spectral density (PSD) of cable M26. Here, X refers to the horizontal direction and Y is perpendicular to the X and longitudinal axes. It can be seen that the vertical acceleration is larger than the horizontal component. The PSD curves clearly show the peaks, which indicate the natural frequencies of the cable. However, the lowest frequency is not clearly identified.

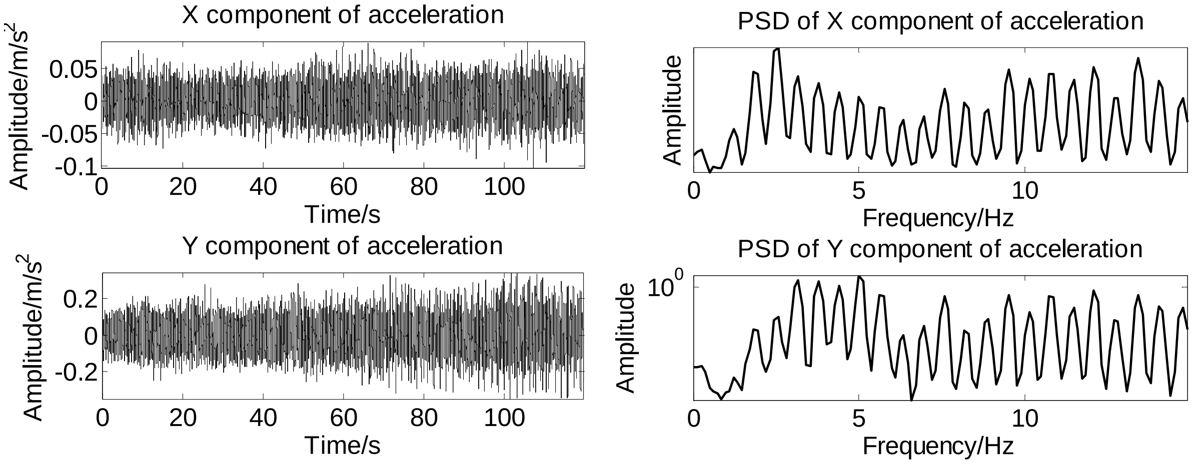

Fig. 4 Acceleration responses and PSD of cable M26

For the same cable, the displacement response measured by the video camera is illustrated in Fig. 5, together with the PSD. Similar to Fig. 4, the measured vertical displacement is larger than the horizontal component, although both are not significant. The measurement has a small drift in the vertical displacement. Nevertheless, the PSD curves clearly show the natural frequencies of the cable. The first three frequencies are 0.65, 1.26, and 1.89 Hz.

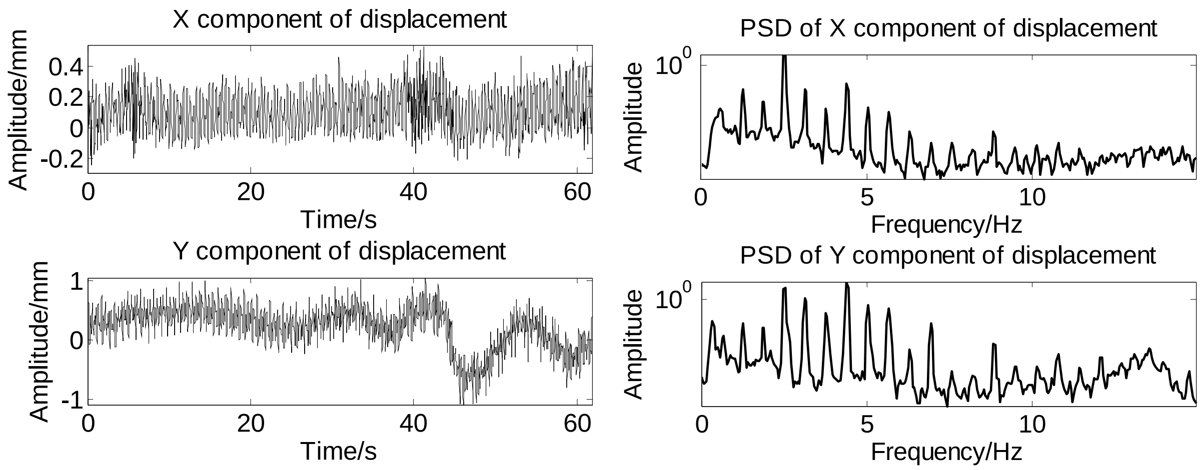

Fig. 5 Displacement responses and PSD of cable M26

Cable S25 was also measured and the acceleration and displacement responses are illustrated in Figs. 6 and 7, respectively. Similar to cable M26, the displacement PSD data has more noise than the acceleration counterpart, while the former has clearer peaks in the low frequency range. The displacement of the cable shows a clear beating phenomenon in Fig. 8. The reason for this requires further study.

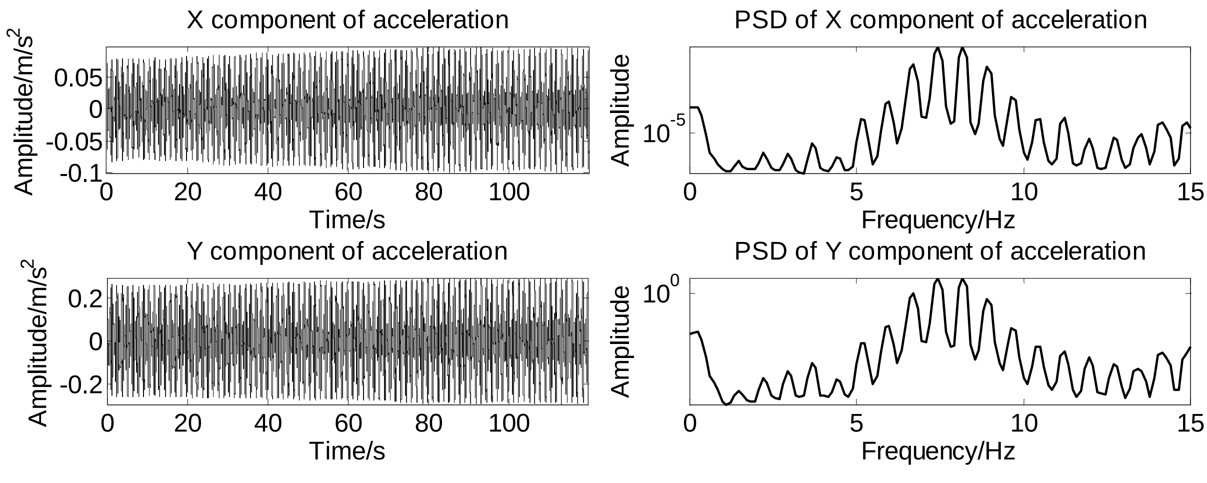

Fig. 6 Acceleration responses and PSD of cable S25

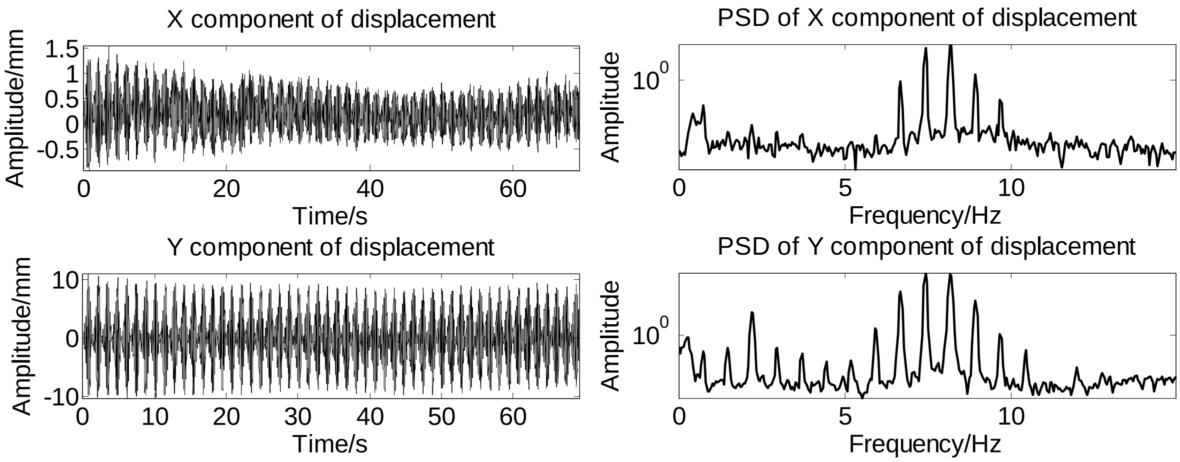

Fig. 7 Displacement responses and PSD of cable S25

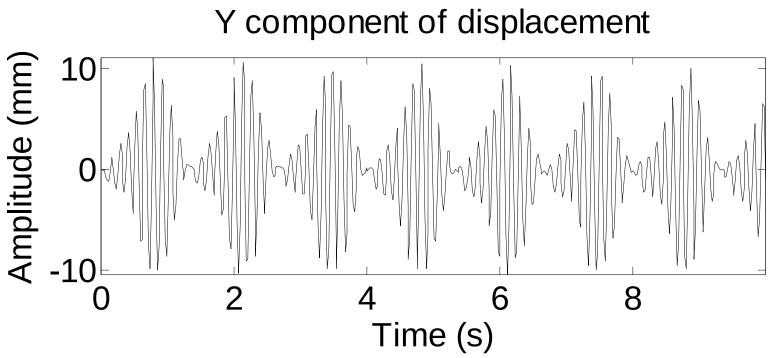

Fig. 8 Beating phenomenon in the displacement of cable S25

The acceleration data measured by the accelerometers are integrated twice to obtain the displacement. Fig. 9 compares the displacement of the cable as measured by the video camera and the results of the double integration of the corresponding acceleration, in both directions. For comparison, only the first few seconds of data are plotted here. It can be seen that the results agree very well for the displacement in the Y direction, the amplitude of which is about 10 mm. The results with small amplitude (0.5 mm) in the X direction reveal some differences.

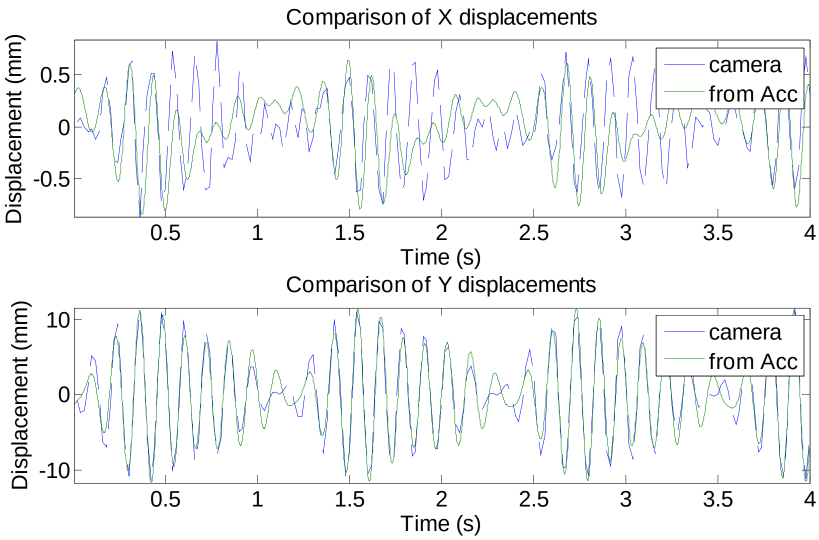

Fig. 9 Comparison of the displacement of cable S20 as measured by the video camera and the accelerometer

TENSION FORCE

The frequencies of the cable, identified from the PSD of the vibration, can be employed to calculate the tension force using empirical formulae. If the effects of sag and bending rigidity are not considered, the relation between the tension force (T) and the first frequency (f_1) is [12]

$$T = 4ml^2 f_1^2 \tag{1}$$

where m is the mass per unit length (kg/m) and l is the length of the cable.

When the sag effect is considered, Eq. (1) can be corrected as [13-14]

$$T = 4ml^2 f_1^2 \bigg/ \left(1 + \frac{1}{2}\left(\frac{2}{\pi}\right)^4 \lambda^2\right) \tag{2}$$

where $\lambda = \dfrac{mg\cos\theta l}{T_0} \bigg/ \sqrt{\dfrac{T_0}{E_{eq}A_c}}$ is the Irvine parameter, T_0 is the initial tension, θ is the angle between the cable axis and the bridge girder, A_c is the cross sectional area of the cable, and $E_{eq} = \dfrac{E}{1 + \dfrac{(mgl\cos\theta)^2 EA_c}{12{T_0}^2}}$ is the equivalent modulus.

When the sag and bending rigidity effects of the cable are both considered, empirical formulae [15] have been developed according to the magnitude of the sag.

1) For a small sag ($\Gamma \geq 3$), the first in-plane frequency (f_1) is used to calculate the tension force as

$$T = 4m(f_1 l)^2 \left[0.828 - 10.5 \left(\frac{C}{f_1} \right)^2 \right] \qquad 0 \leq \xi \leq 6 \tag{3a}$$

$$T = 4m(f_1 l)^2 \left[0.865 - 11.6 \left(\frac{C}{f_1} \right)^2 \right] \qquad 6 \leq \xi \leq 17 \tag{3b}$$

$$T = 4m(f_1 l)^2 \left[1 - 2.20 \frac{C}{f_1} - 0.550 \left(\frac{C}{f_1} \right)^2 \right] \qquad \xi \geq 17 \tag{3c}$$

2) For a large sag ($\Gamma \leq 3$), the second in-plane frequency (f_2) is used

$$T = m(f_2 l)^2 \left[0.882 - 85.0 \left(\frac{C}{f_2} \right)^2 \right] \qquad 0 \leq \xi \leq 17 \tag{4a}$$

$$T = m(f_2 l)^2 \left[1.03 - 6.33 \frac{C}{f_2} - 1.58 \left(\frac{C}{f_2} \right)^2 \right] \qquad 17 \leq \xi \leq 60 \tag{4b}$$

$$T = m(f_2 l)^2 \left[1 - 4.40 \frac{C}{f_2} - 1.10 \left(\frac{C}{f_2} \right)^2 \right] \qquad \xi \geq 60 \tag{4c}$$

where $\Gamma = \sqrt{\frac{mgl}{128 EA \delta^3 \cos^5 \theta} \cdot \frac{0.31\xi + 0.5}{0.31\xi - 0.5}}$, $\xi = l\sqrt{\frac{T_0}{EI}}$, $C = \sqrt{\frac{EI}{ml^4}}$, $\delta = \frac{s}{l_0} = \frac{d}{l} \cdot \frac{1}{\cos^2 \theta}$, and

$$d = \frac{wl^2}{8T} \left[1 - \frac{8}{\xi^2} \left(1 - \sec h \frac{\xi}{2} \right) \right].$$

The parameters and first frequencies of the cables are listed in Table 1. Based on the above equations, the tension forces are calculated and listed in Table 2. Compared with those measured in 2008 before the bridge was put into service, the tension forces vary from −6% to 12%, possibly due to load redistribution. Nevertheless, the tension forces are regarded as in the safe region.

Table 1 Parameters of the cables

No.	m (kg/m)	θ (rad)	l (m)	Radius (m)	E *(Pa)*	A_c (m^2)	f_1 (Hz)	f_2 (Hz)
S20	81.7	0.5189	163.068	0.143	2E+11	9.737E-03	0.8423	1.685
S25	91.3	0.5274	182.515	0.151	2E+11	1.089E-02	0.7477	1.480
S26	91.3	0.5303	186.430	0.151	2E+11	1.089E-02	0.7019	1.404
M26	85.9	0.4506	206.434	0.148	2E+11	1.020E-02	0.6256	1.251
M25	85.9	0.4568	199.545	0.148	2E+11	1.020E-02	0.7140	1.389
M24	85.9	0.4633	191.494	0.148	2E+11	1.020E-02	0.6866	1.389

Table 2 Tension of the cables

No.	S20	S25	S26	M26	M25	M24
T (kN)	6032.7	6662.4	6123.1	5730.7	6851.4	5821.1
T (kN) in 2008	6144.7	6633.0	6323.0	5923.0	6099.0	6179.0
Error (%)	-1.96	0.44	-3.16	-3.25	12.34	-5.79

CONCLUSIONS

Although dynamic displacement is an important parameter in many applications, low cost, accurate measurement techniques are still not available. In this paper, a videogrammetric technique using a home-use digital video camera is developed to measure the dynamic displacement of cables. This preliminary study shows that the proposed videogrammetric technique is a potentially promising method of measuring the vibration of structures.

The accuracy of the measurement using this approach heavily depends on the camera resolution, the distance between the camera and the targeted structure, the frequency of the movement, and the climatic conditions. The video camera used in this study has a resolution of 640 × 480 pixels. If the target moves within a range of 64 mm, then the camera can achieve a resolution of about 0.1 mm. If a high-definition video camera (1920 × 1120 pixels) is used, the accuracy will be improved by two to three times. The climatic conditions do affect the video quality and, as a result, the image recognition.

The new technique can be used in the monitoring of cables in cable-stayed bridges, the main cables in suspension bridges, transmission lines, and other types of cable structure. With appropriate modification, it can also be applied to monitor other components of structures, for example, the decks of bridges or high-rise buildings.

ACKNOWLEDGMENTS

The authors gratefully acknowledge the financial support provided by Research Grants Council of the Hong Kong Special Administrative Region of China (Project No. PolyU 5298/11E) and the Hong Kong Polytechnic University (Project No. A-PD0H).

REFERENCES

[1] Abe M, Fujino Y, Kaito K (2001) Damage detection of civil concrete structures by laser Doppler vibrometry [C]. Proceedings of the 19th International Modal Analysis Conference, Kissimmee, Florida, USA, pp. 704-709

[2] Kaito K, Abe M, Fujino Y (2001) An experimental modal analysis for RC bridge decks based on non-contact vibration measurement [C]. Proceedings of the 19th International Modal Analysis Conference, Kissimmee, Florida, USA, pp. 1561-1567

[3] Bales F B (1985) Close-range photogrammetry for bridge measurement [J]. *Transportation Research Record*, 950: 39-44

[4] Li J C, Yuan B Z (1988) Using vision technique for bridge deformation detection [C]. Proceedings of the International Conference on Acoustic, Speech and Signal Processing, New York, USA, pp. 912-915

[5] Olaszek P (1999) Investigation of the dynamic characteristic of bridge structures using a computer vision method [J]. *Measurement*, 25: 227-236

[6] Patsias S, Staszewski WJ (2002) Damage detection using optical measurements and wavelets [J]. *Structural Health Monitoring*, 1: 7-22

[7] Fu G, Moosa A G (2002) An optical approach to structural displacement measurement and its application [J]. *Journal of Engineering Mechanics*, 128: 511-520

[8] Yoshida J, Abe M, Kumano S, Fujino Y (2003) Construction of a measurement system for the dynamic behaviors of membrane by using image processing [C]. International Conference on Textile Composites and Inflatable Structures, Barcelona, Spain

[9] Chung H, Liang J, Kushiyama S, Shinozuka M (2004) Digital image processing for

non-linear system identification [J]. *International Journal of Non-linear Mechanics*, 39: 691-707

[10] Ji Y F, Chang C C (2008) Non-target image-based technique for bridge cable vibration measurement [J]. *Journal of Bridge Engineering*, 13: 34-42

[11] Wu Q X, Chen B C, Wang W P (2010) Dynamic behaviors of Quanzhou Jinjiang bridge [J]. *Journal of Highway and Transportation Research and Development*, 27(4): 44-50 (in Chinese)

[12] Fujino Y, Warnitchai P, and Pacheco B M (1993) An experimental and analytical study of autoparametric resonance in a 3DOF model of cable-stayed-beam [J]. *Nonlinear Dynamics*, 4: 111-138

[13] Wu Q X, Takahashi K, Okabayashi T, Nakamura S (2003) Response characteristics of local vibrations in stay cables on an existing cable-stayed bridge [J]. *Journal of Sound and Vibration*, 261(3): 403-420

[14] Pinto da Costa A, Martins J A C, Branco F, Lilien J L (1996) Oscillations of bridge stay cables induced by periodic motions of deck and/or towers [J]. *Journal of Engineering Mechanics*, 122: 613–622

[15] Zui H, Shinke T, Namita Y (1996) Practical formulas for estimation of cable tension by vibration method [J]. *Journal of Structural Engineering*, 122(6): 651–656